JOURNAL OF CATALYSIS 21, 122–129 (1971)

Dual-Functional Activities in Nickel Acid Catalysts

JAMES T. RICHARDSON*

Esso Research and Engineering Company, Baytown, Texas 77520

Received July 10, 1970

The specific activity of supported nickel for benzene hydrogenation, ethane and *n*-hexane hydrogenolysis decreases with the increasing acidity of the support in the order of $SiO_2 > Al_2O_3 >$ silica–alumina > Y faujasite; the Y faujasites (Na, Li, Ca, Mg) all have the same activities. The reducibility of 3% nickel faujasites decreases from 100% to zero in the order $NaY \sim LiY > CaY > MgY > NH_4Y = 0$. Specific *n*-hexane isomerization rates increase with acidity so that isomer yields are maximized for CaY.

There are two types of sites on nickel. Site I (35%) promotes hydrogenolysis, Site II (65% weaker than Site I) hydrogenation–dehydrogenation. There is no evidence for synergistic influences between metal and acid sites.

Introduction

Catalytic dual-functionality is used extensively in commercial processes such as hydrocracking and reforming. In addition, the unintentional presence of secondary catalytic components, such as metal poisons on cracking catalysts, often plays an important role in establishing selectivity factors. A thorough understanding of the interrelation between the different types of activities is essential for the design of novel and more efficient catalytic operations. The present state of knowledge has been reviewed extensively (*1–3*) and many research reports devoted to this subject appear in this and other journals.

One of the most widely used systems is nickel dispersed on various acid supports, in spite of susceptibility to sulfur poisoning. Several definitive yet conflicting patterns are beginning to emerge. Taylor and Staffen (*4*), Yates *et al.* (*5*), Taylor *et al.* (*6, 7*), Carter *et al.* (*8, 9*) reported that benzene hydrogenation, cyclopropane hydrogenation, and ethane hydrogenolysis over Ni–SiO_2, Ni–Al_2O_3 and Ni–silica–alumina show different intrinsic activities depending upon the support used. Ethane hydrogenolysis is also sensitive to nickel crystallite size. Shephard (*10*), working with propane hydrogenolysis, also showed crystallite size effects for Ni–Al_2O_3. Aben *et al.* (*11*), however, reported benzene hydrogenation to be independent of support and particle size.

Several hypotheses have been advanced to explain these observations. These include metal-support electronic interactions, support-induced morphology differences, molecular inaccessibility through metal-support compounds, and microporosity. These possibilities raise an interesting fundamental question in the use of nickel for dual functional reactions. Namely, do the metallic activity (M) of the nickel and the acidic activity (A) of the support function in a purely additive way to give a combined activity of ($M + A$), or is there a dependence of M on A and/or A on M so that the final activity is better represented by ($M + A + MA$)? Thus, the factors in SiO_2, Al_2O_3 and silica–alumina which establish the acidic properties might also play a part in altering the hydrogenation activity of the nickel. The analysis of the direct interplay between acidity and hy-

* Present address: Department of Chemical Engineering, University of Houston, 3801 Cullen Boulevard, Houston, Texas 77004.

drogenation is complicated by the structural and morphological factors inherent in the different chemical and physical properties of the support.

Obviously, a series of supports with essentially the same chemical nature, similar morphology and porosity, containing the same amount of identical nickel crystallites but exhibiting a wide range of acidic behavior is necessary in order to clarify these points. Faujasites, cation-exchanged to yield different acidities (*12*, *13*), fill this need.

The results reported below show that the hydrogenation activity and acidic activity in the nickel–faujasite system are independent of each other, with no mutual enhancement of the overall dual-functional activity. However, there is a dependence of nickel reducibility on the cation present with a subsequent effect on yields. Furthermore, the results of Sinfelt and co-workers have been confirmed and included in this comparison. Metal poisoning experiments suggest site heterogeneity on the nickel.

Experimental Methods

1. Catalysts

Samples of Na, Li, Ca, Mg, and NH_4 faujasites were back-exchanged with nickel nitrate solution to give approximately 3 wt % nickel, measured by chemical analysis. The catalysts were thoroughly washed after each exchange to insure that no excess nickel remained. The usual drying procedures were carried out at 100°C in N_2 before reduction and use.

Samples of Ni–SiO_2, Ni–Al_2O_3 and Ni–silica alumina were prepared by impregnating high purity silica, γ-Al_2O_3 and Davisson DA-1 cracking catalyst with enough nickel nitrate solution to give 5% nickel. Similar drying and reduction treatments were used.

2. Pretreatment

All catalysts were reduced in the reactor with flowing hydrogen for 16 hr at 400°C. Samples of the same catalyst were reduced under the same conditions in a Faraday magnetization apparatus described elsewhere (*14*). Typical results of magnetization versus magnetic field following this reduction are given in Fig. 1. The saturation magnetization, σ_∞, was obtained from the empirical expression (*15*),

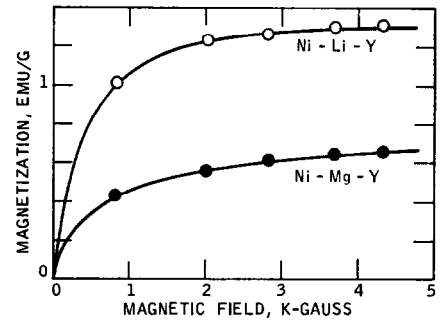

FIG. 1. Magnetization versus magnetic field for Ni–Li–Y and Ni–Mg–Y.

$$\frac{1}{\sigma} = \frac{1}{\sigma_\infty} + \frac{1}{\sigma_\infty(\alpha H)^{0.9}}, \qquad (1)$$

from which the weight fraction of reduced nickel was calculated, using

$$\omega = \frac{\sigma_\infty}{55.5} \qquad (2)$$

Also, an estimate of the particle size was made from (*16*)

$$d^3 = \frac{18kT}{\pi IH}\left[\frac{\sigma(H)}{\sigma(\infty)}\right], \qquad (3)$$

where d is the average particle diameter, I the spontaneous magnetization of bulk nickel, T the temperature and k the Boltzman constant.

3. Catalytic Activity

Four test reactions were used; cumene cracking (*12*) to characterize acidic activity, benzene hydrogenation, and ethane hydrogenolysis to measure metallic hydrogenation activity, and n-hexane isomerization as an index to dual-functional activity. The same flow reactor was used for each reaction but with fresh samples for each run. Activity was calculated from the conversion after 1 hr at a standard temperature and flow rate, predetermined to give measurable yet small conversions. Appropriate chromatographic columns were used

to analyze the reactor tail gas for the products of each particular reaction.

Helium was passed through a cumene saturator as the feed for cumene cracking; hydrogen saturated with benzene and *n*-hexane was used for benzene hydrogenation and *n*-hexane isomerization, respectively. A mixture of hydrogen and ethane was used for ethane hydrogenation. The exact conditions are given in Table 1.

The faujasite series shows a decrease in reduced nickel as the acidity increases. The crystallite sizes decreases slightly with increased acidity but not in any significant manner. Rabo *et al.* (*17*) have studied the reducibility of Ni^{2+} ions in Ca–Y faujasite by alkali metals. They concluded that nickel ions located in the S_I positions (interior, sixfold coordination with oxygen ions) are harder to reduce than those in the S_{II} positions (surface of the supercage, threefold coordination with oxygen ions). Furthermore, nickel prefers the S_I to the S_{II} position. There are 16 S_I positions in a unit cell of Y faujasite. The samples in this investigation contain approximately 3 wt % nickel or 5–6 atoms/unit cell. There are sufficient locations to satisfy all of the nickel ions in S_I positions.

TABLE 1

AMOUNT, EXTENT OF REDUCTION, AND MAGNETIC PARTICLE SIZE FOR NICKLE ON ACID SUPPORTS

Support	Wt % Ni	Wt % Ni reduced	Crystallite diam (Å)	Surface area[a] (m^2/g of Ni reduced)
SiO_2	5.00	4.95	95	69
Al_2O_3	5.03	0.63	79	86
Silica–alumina	4.89	3.68	83	81
Na–Y	2.46	2.46	126	54
Li–Y	3.03	2.41	112	59
Ca–Y	3.05	2.31	99	66
Mg–Y	2.68	1.21	95	70
NH_4–Y	2.40	0	—	

[a] Calculated from the Ni crystallite diameter.

Reaction rates were determined from:

$$\text{rate} = \left[\frac{F}{\omega}\right] \times (\text{Conversion}), \qquad (4)$$

where F is the feed rate in moles per minute and ω is the weight fraction of reduced nickel.

In the few cases where conversion was high enough so that differential conditions did not apply, an average feed rate, based on entrance and exit concentrations, was used in Eq. (4).

RESULTS AND DISCUSSION

Results of the magnetic measurements of reducibility and crystallite size are given in Table 1. The small amount of reduced nickel on γ-Al_2O_3 is not surprising in view of the formation of nonreducible $NiAl_2O_4$ under these conditions (*15*, *16*). Silica–alumina also complexes a smaller amount of the nickel in a nonreducible form. All of the nickel on silica is reduced but the nickel area is less than that obtained by Taylor *et al.* (*6*).

It is tempting to hypothesize that the decreased reducibility of the nickel ions is due to an increase in the nickel S_I concentration as the acidity increases. However, this is contrary to electrostatic and other considerations which predict that the Na–faujasite would exchange with a greater number of nickel ions in the S_I position than the Mg–faujasite.

These observations may reflect a decreasing accessibility or affinity for hydrogen of the nickel in the S_{II} position. However, the effective charge of the nickel is expected to increase as the neighboring cations increase in charge/size ratio (e/r), exerting a greater electron attraction on the nickel–oxygen bonds (*12*, *18*). This in-

crease in electron affinity from Ni–Na–Y to Ni–Mg–Y should result in an increased nickel reducibility. Predictions based on size factors alone show a similar tendency. Thus, hydrogen accessibility and activation is not a reasonable hypothesis.

The formation of nickel particles approximately 100 Å in diameter on the exterior of the faujasite crystallites must entail a mobile intermediate species such as Ni^0, Ni^{1+} or Ni–H. A decrease in mobility of this species as the overall cavity polarization increases may be a factor in controlling the decreased reduction. Further investigative attempts at detecting these intermediates and clarifying the exact mechanism of nickel reduction in faujasites will be necessary in order to resolve these points.

The possibility that the nickel is indeed fully reduced but exists in crystallites too small to be detected magnetically must be considered. Figure 2 shows that the benzene conversion is directly dependent on the amount of reduced nickel, decreasing to zero for the Ni–NH_4–Y faujasite. If the nickel were present as a highly dispersed nickel, the benzene activity would remain the same, if not increase. Similar effects were noted for ethane hydrogenolysis and *n*-hexane conversion. Furthermore, Yates (*19*), working with this same Ni–NH_4–Y faujasite, found no hydrogen adsorption characteristic of reduced nickel. The possibility of undetected nickel particles need not be considered.

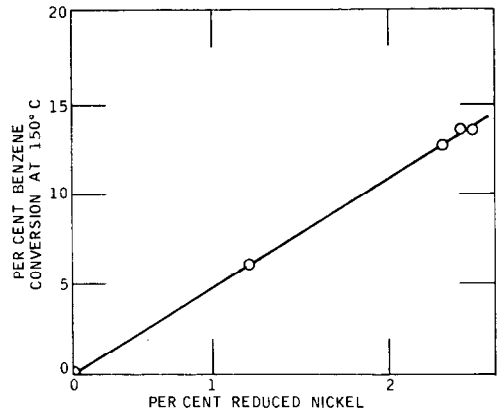

FIG. 2. Benzene hydorgenation dependence on the amount of reduced nickel in the faujasites.

Results of the catalytic activity measure-

TABLE 2

CATALYTIC ACTIVITY MEASUREMENTS

Reactor length, 2.2 cm; reactor diam, 0.5 cm; pressure, 1 atm; particle size, 60μ.

Reaction:	Cumene dealkylation	Benzene hydrogenation	Ethane hydrogenolysis	*n*-Hexane isomerization
Temp (°C):	300	150	300	300
Catalyst w (g):	0.600	0.600	0.600	0.600
Flow rate (cm^3/min):	25	13	20	20
Feed rate (moles/min):	2.85×10^{-5}	3.11×10^{-5}	2.17×10^{-4}	8.78×10^{-5}

		Conversions (mole %)				
					n-Hexane	
Support	Wt % Ni reduced				Hydrogenolysis	Isomerization
SiO_2	4.96	0.2	>100	>100	>100	0
Al_2O_3	0.63	0.7	54.3	—	28.1	0
Silica–alumina	3.68	1.0	75.8	18.1	20.0	0.1
Na–Y	2.46	4.0	13.5	3.3	12.3	.6
Li–Y	2.41	32	13.5	2.8	13.6	1.0
Ca–Y	2.31	40	12.7	3.0	13.4	8.0
Mg–Y	1.21	53	6.1	2.0	6.0	5.0
NH_4	0	88	0	0	0	0

ments are given in Table 2. Cumene dealkylation is a useful index for acid activity (*12*) even though the exact interrelation is not known. The Ni–Y faujasites show the expected increase in cumene conversion as the cation changes from Na to NH_4. There is an increase over the conversion observed for the samples without nickel (*12*) due to the effect of the Ni^{2+} ions themselves. The synergistic enhancement displayed by the Cu–faujasite system (*12*) was not present, however. Reduction with hydrogen resulted in a further increase in cumene conversion, promoted by the proton sites left behind when the nickel ions were removed. This effect was not significant and did not alter the dependence of acidity on the cation. The cumene conversion is used, hereafter, as an acidity parameter in order to compare the behavior of the various supports.

Benzene hydrogenation and ethane hydrogenolysis both reflect the activity of the metallic component. As discussed above, there is disagreement on whether or not the activities per unit surface of metal are constant, or dependent on the support. Table 2 shows a wide variation of both these conversions as the support varies from SiO_2 to NH_4–Y. For the faujasites, the extent of reduction will naturally influence the results. The intrinsic rates (Table 3) of the faujasites are approximately constant for both these reactions. They were averaged and compared in Table 4 with the results of Taylor and Staffin (*4*), Yates *et al.* (5), Taylor *et al.* (*6*, *7*), and Carter *et al.* (*8*, *9*) for SiO_2 and silica–alumina supports. The agreement is fairly good considering these were different preparations and process conditions. The trends are the same in the three sets of measurements. When compared with the faujasites in this study, there is a definite effect, SiO_2 > silica alumina > faujasite. Since this is also the direction of increasing acidity, the specific rates (per gram of reduced nickel) are plotted in Fig. 3 as a function of cumene conversion. Figure 3 is not intended to imply that there is a dependence of these rates on the acidity of the support (thus indicating some dual-functional mechanism) but merely demonstrates the large differences observed by the metals under the influence of these supports. If these differences are related to the structure or morphology induced by the support, then Fig. 3 shows

TABLE 3
REACTION RATES FOR BENZENE HYDROGENATION AND ETHANE HYDROGENOLYSIS ON Ni–FAUJASITE CATALYSTS

	Rates (moles/min/m² reduced Ni)	
Support	Benzene hydrogenation (150°C) ($\times 10^6$)	Ethane hydrogenolysis (300°C) ($\times 10^6$)
NaY	5.26	8.93
LiY	4.92	7.08
CaY	4.32	7.05
MgY	3.73	8.36
NH_4Y	—	—

TABLE 4
COMPARISON OF RESULTS WITH PREVIOUS MEASUREMENT

	Rates (moles/min/m² Ni) (reduced)		
Support: Reaction	SiO_2	Silica–alumina	Y–Faujasites
Benzene hydrogenation (150°C)			
This study	1.64×10^{-4}[b]	1.32×10^{-5}	4.56×10^{-6}
Ref. (*4*)	0.71×10^{-4}[b]	2.18×10^{-5}	—
Ethane hydrogenolysis (300°C)			
This study	5.48×10^{-4}[b]	2.20×10^{-5}	7.86×10^{-6}
Ref. (*6*)	1.03×10^{-4}[a]	1.74×10^{-6}[a]	—

[a] Extrapolated to these conditions using the kinetic parameters given by authors.
[b] Extrapolated from lower temperature data.

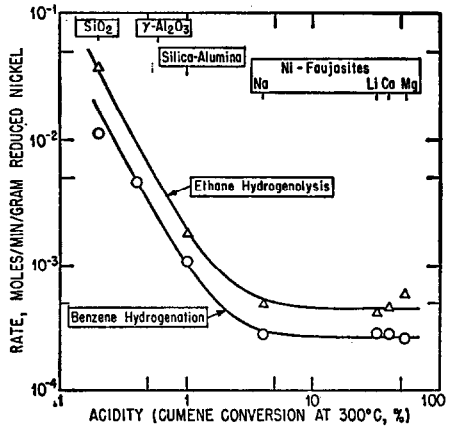

FIG. 3. Benzene hydrogenation and ethane hydrogenolysis over nickel as a function of support acid activity.

that the faujasite series does indeed yield identical crystallites of nickel, although different from those of the other materials. If, however, the variations are due to an induction from some surface property that also affects the acidity, then this influence is only important at low acidities and the metal is insensitive in the acid strength range represented by the faujasites.

The dual-functional mechanism for *n*-hexane isomerization has been reviewed extensively (*2*) and is shown in Fig. 4. The terminology suggested by Weisz (*2*) to differentiate between "hydrogenolysis" (cracking on *M* sites) and "hydrocracking" (cracking on *A* sites) has been adopted. Typical product distributions are shown

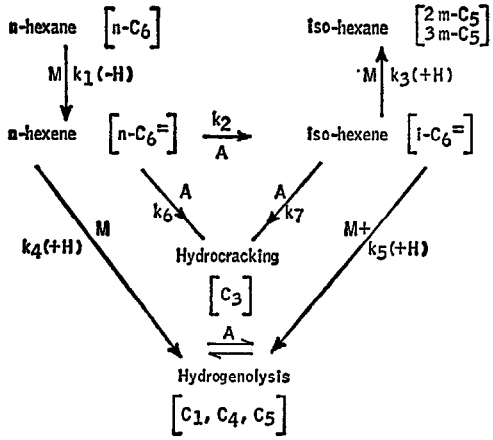

FIG. 4. Dual-functional mechanism for *n*-hexane isomerization.

TABLE 5
H_2S POISONING ON Ni–Li–Y FAUJASITE

Product	*n*-Hexane hydrogenolysis and isomerization (moles/100 moles of nC_6 H_2S cm³				
	0	0.05	0.10	0.15	0.2
C_1	56.5	32.8	—	—	—
C_2	—	—	—	—	—
C_3	0.89	2.10	0.64	0.25	0.20
iC_4	0.05	0.23	—	—	—
nC_4	1.63	2.69	—	—	—
iC_5	0.24	0.53	—	—	—
nC_5	2.33	3.43	—	—	—
2MP	0.62	1.66	3.43	2.42	1.01
3MP	0.32	1.42	0.84	0.66	0.49
nC_6	85.5	91.2	95.4	96.7	—

in Table 5. The isomerization rate is taken to be the rate of conversion of *n*-hexane to the isomers 2-methylpentane and 3-methylpentane. The hydrogenolysis rate accounts for the excess conversion of *n*-hexane over isomerization although this also includes the "hydrocracking" formation of propane. No olefins were detected in the product.

Figure 5 shows the variation of both these rates with support acidity. Silica and alumina promote hydrogenolysis only, with the hydrogenolysis rate decreasing to a constant value for the silica–alumina and faujasites. This is similar to the behavior of benzene and ethane. The isomerization rate increases with acidity as expected, but there is a large variation over the faujasite range. This isomerization reflects the total

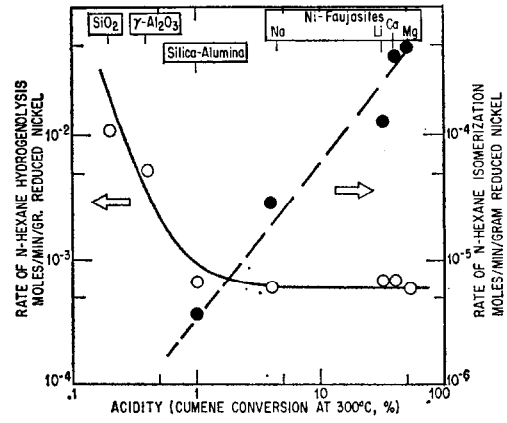

FIG. 5. *n*-Hexane hydrogenolysis and isomerization over nickel as a function of support acid activity.

effect of steps k_1, k_2, and k_3 in Fig. 4 but responds mostly to increases in k_2, since k_1 and k_3 remain constant. The balance between increasing isomerization and a decreasing amount of reduced nickel results in the optimum yield of isomerization shown in Table 2 for Ni–Ca–Y. Thus, there is no evidence to support any dependence of M on A or A on M.

In order to confirm and further elucidate this last conclusion, samples of Ni–Li–Y were progressively poisoned with doses of H_2S during cumene, benzene, and n-hexane conversion measurements. Figure 6 shows the response of the acid and metal activities to H_2S poisoning. The cumene dealkylation remains the same, whereas the benzene hydrogenation conversion decreases to zero with increasing sulfur poisoning. Thus, the H_2S does not affect the acid but progressively poisons the metal sites. The benzene hydrogenation curve in Fig. 6 would result if either the nickel surface were poisoned uniformly or the bed were selectively deactivated with a sulfided zone moving down the reactor. However, the results shown in Fig. 7 for the n-hexane conversion clearly indicate that uniform surface poisoning is taking place. The fresh catalyst converts 93% of the n-hexane via the hydrogenolysis route. Figure 7 shows that this activity is rapidly deactivated by H_2S, resulting in an increase of the isomerization rate. This implies that the intermediate isohexenes are competitively cracked by hydrogenolysis on the most active sites of the nickel. These active sites (Type I) account for approximately 35% of the metallic sites. The Type I sites are poisoned after the second dose of H_2S. The remaining sites (Type II, weaker than Type I) show almost exclusively isomerization activity with only a small amount of hydrocracking. Subsequent poisoning results in a continuing decrease of both isomerization and hydrocracking. The catalyst is completely poisoned after 0.25 ml of H_2S. Assuming all the H_2S is adsorbed and using the nickel area given in Table 1, this corresponds to one sulfur atom adsorbed for every two surface nickel atoms. This is in agreement with the results of Selwood (*20*), demonstrating the internal consistency of this interpretation of magnetic particle size and sulfur poisoning. Benzene hydrogenation is poisoned at the same H_2S dosage and must accordingly take place on Type II sites. This is not surprising since the k_1, k_3 step for isomerization involves dehydrogenation–hydrogenation mechanism on Type II.

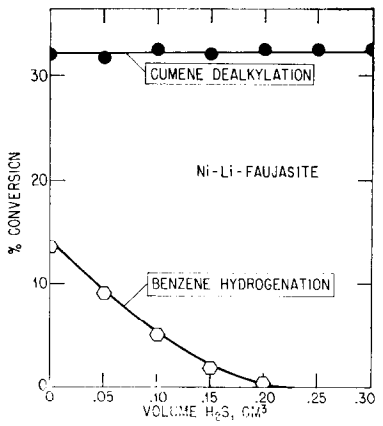

FIG. 6. Effect of H_2S poisoning on metal and acid functions.

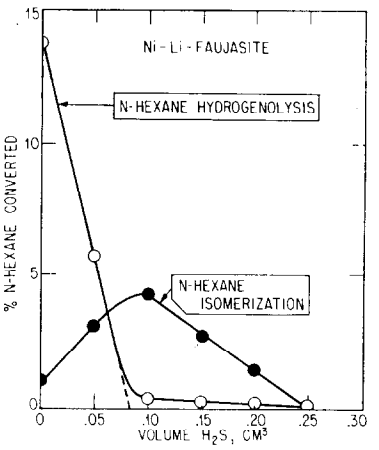

FIG. 7. Effect of H_2S poisoning on n-hexane hydrogenolysis and isomerization.

CONCLUSIONS

The conclusions from this investigation are as follows:

1. The specific activity of reduced nickel for benzene hydrogenation, ethane and n-hexane hydrogenolysis decreases with the

increasing acidity of the support in the order $SiO_2 > Al_2O_3 >$ silica–alumina > Y faujasites, *but* these activities remain constant in the faujasite acidity range from Na–Y to Mg–Y.

2. The specific *n*-hexane isomerization activity of the nickel-support increases with increasing support acidity.

3. The reducibility of the nickel ion-exchanged at the 3 wt % level decreases in the faujasite series, NaY to NH_4–Y.

4. The net effect of (2) and (3) is to maximize the isohexane yield at Ni–Ca–Y.

5. There are two types of sites on nickel supported by faujasite. Type I, the most active, accounts for 35% of the total surface and is responsible for *n*-hexane hydrogenolysis. Type II is responsible for *n*-hexane isomerization, hydrocracking, and benzene hydrogenation.

6. Hydrogen sulfide poisons Type II sites with one sulfur for every two nickel atoms.

7. There is no evidence of other than simple additive behavior in the dual-functioned activity of nickel and faujasite acidity.

References

1. Ciapetta, F. G., Dobres, R. M., and Baker, R. W., "Catalysis," Vol. 6, p. 495. Reinhold, New York, 1958.
2. Weisz, P. B., "Advan. Catal. Relat. Subj." 13, 137 (1962).
3. Emmett, P. H., Sabatier, P., and Reid, E. E., "Catalysis Then and Now." Franklin Pub., Palisade, N. J., 1965.
4. Taylor, W. F., and Staffin, H. K., *Trans. Faraday Soc.* **63**, 2309 (1967).
5. Yates, D. J. C., Taylor, W. F., and Sinfelt, J. H., *J. Amer. Chem. Soc.* **86**, 2996 (1964).
6. Taylor, W. F., Yates, D. J. C., and Sinfelt, J. H., *J. Phys. Chem.* **68**, 2962 (1964).
7. Taylor, W. F., Sinfelt, J. H., and Yates, D. J. C., *J. Phys. Chem.* **69**, 3857 (1965).
8. Carter, J. L., Cusumano, J. H., and Sinfelt, J. H., *J. Phys. Chem.* **70**, 2257 (1966).
9. Carter, J. L., and Sinfelt, J. H., *J. Phys. Chem.* **70**, 3033 (1966).
10. Shephard, F. E., *J. Catal.* **14**, 148 (1960).
11. Aben, P. C., Platteeuw, J. C., and Southamer, B., *Proc. Int. Congr. Catal., 4th, Moscow, 1968,* Prepr. No. 31.
12. Richardson, J. T., *J. Catal.* **9**, 182 (1967).
13. Richardson, J. T., *J. Catal.* **9**, 172 (1967).
14. Richardson, J. T., and Beauxis, J. O., *Rev. Sci. Instrum.* **34**, 877 (1963).
15. Schuit, G. C. A., and Van Reijen, L. L., *Advan. Catal. Relat. Subj.* **10**, 243 (1958).
16. Trzebiatowski, W., "Catalysis and Chemical Kinetics." Academic Press, New York (1964).
17. Rabo, J. A., Angell, C. L., Kasia, P. H., and Schomaker, C., *Chem. Eng. Progr.* **63**, 31 (1967).
18. Richardson, J. T., *J. Catal.* **9**, 178 (1967).
19. Yates, D. J. C., private communication.
20. Selwood, P. W., "Adsorption and Collective Paramagnetism." Academic Press, New York, 1962.